JOURNAL OF MATERIALS SCIENCE 29 (1994) 2916–2920

Interlaminar fracture of carbon–thermoplastic polyimide composites

JIANG ZHOU, TIANBAI HE, JIN ZHANG, MENGXIAN DING
Polymer Physics Laboratory, Changchun Institute of Applied Chemistry, Chinese Academy of Sciences, Changchun 130022, People's Republic of China

Mode I interlaminar fracture of a novel amorphous thermoplastic polyimide reinforced with unidirectional carbon fibre has been studied experimentally using double cantilever beam specimens and scanning electron microscopy. Three kinds of composite were manufactured from different monomeric reactant solutions which were prepared by using different alcohol solvents. The values of fracture toughness of these three composites were measured to construct the crack growth resistance curves (R curves). The contributions from various failure processes to the total fracture toughness were separated, and approximate calculations of these contributions were conducted based on several simplifying assumptions and some data obtained from the fracture surfaces. Though fibre peeling and fibre breakage are observed, interlaminar fracture in the composites studied is primarily controlled by fracture and deformation in the matrix. It is found that the measured fracture toughnesses of the composites differ from each other not only in the propagation values but also in the initial values. A possible reason for this may be variations of matrix ductility in the three composites.

1. Introduction

Fibre-reinforced resin matrix composites are now being used as structural materials in the aircraft and aerospace industries. The structural performance of a fibre-reinforced composite depends on its ability to resist delamination or interlaminar crack initiation and propagation, because delamination can lead to a loss of stiffness and strength of a structure. Thus, a knowledge of the interlaminar crack growth behaviour is essential for material development and selection as well as for design and life prediction studies. A commonly utilized approach to characterize the propagation of interlaminar cracks is through the application of linear elastic fracture mechanics (LEFM), which enables the critical strain energy release rate or fracture toughness G_c to be deduced [1–6].

In many applications within the aerospace industry, elevated long-term use temperatures are required. Up to now thermosetting composites have dominated these applications. However, thermosets are inherently brittle, and the concern is that the brittle resin between laminates may be easily damaged by impact loads to initiate cracks and delaminations. Thus, the matrix material plays an important role in the fracture behaviour and toughness of these materials. In order to improve the fracture toughness of polymer composites, some studies have been directed towards increasing the toughness of the thermoset [7]. High-temperature thermoplastics which are less brittle than thermosets are also being introduced.

Polyimides have outstanding thermal stability and are relatively easy to fabricate, which makes this resin system competent as a matrix for advanced composites. Recently, a new amorphous thermoplastic polyimide (PTI) has been developed in this laboratory. In order to examine this high-temperature resin as a composite matrix, continuous carbon fibre composites were prepared via solution impregnation. However, the PTI resin requires the use of organic solvents such as N,N-dimethylformamide and N,N-dimethylacetamide for impregnation of fibres, and the high viscosity results in difficulty in impregnation. Fortunately the monomers for PTI are soluble in alkyl alcohol solvents, so the polymerization of monomeric reactants (PMR) approach is used to manufacture composites based on PTI. This is expected not only to reduce environmental problems but also to improve the processability in steps such as impregnating and moulding.

Since a number of alcohol solvents can be used to prepare the monomeric reactant solution, it is necessary to compare the properties of composites produced by using different reactant solutions. The work presented in this paper investigates and characterizes the fracture behaviour of three kinds of composite based on PTI. These composites were made from prepregs which were manufactured via fibre impregnation in three different reactant solutions. At the same time the micromechanisms of interlaminar cracking is also studied for the purpose of attaining a greater understanding of the fracture behaviour of thermoplastic composites.

2. Experimental procedure

2.1. Material preparation

A proprietary method was used to produce the materials in this study. Aromatic dianhydride and aromatic

0022–2461

diamine, according to a certain mole ratio, were dissolved in three different alcohol solvents to obtain three kinds of PMR-type reactant solution. We defined these solutions as A, B and C. The solids content was 40% in A and C and 30% in B. Impregnation of the carbon fibres (CTU4) was performed on a small-scale winding machine. Two metering bars were used to remove excess resin and to maintain a fibre volume content of about 50% in the prepregs. After the solvents in prepregs were evaporated in an oven the prepregs were cut into 120 mm by 170 mm plies, stacked unidirectionally, and then put in a vacuum oven to complete condensation to form the thermoplastic polyimide PTI. Finally, these laid-up materials were placed in a hot press for consolidation. In order to distinguish the materials produced from solutions A, B and C, the panels made from the prepregs were designated CTU4/PTI (A), CTU4/PTI (B) and CTU4/PTI (C), respectively. Samples for tests of interlaminar fracture, interlaminar shear strength and dynamic mechanical analysis of the three materials were machined from the panels.

2.2. Interlaminar fracture tests

The double cantilever beam (DCB) testing geometry was used in the present fracture investigations. All specimens were 20 mm in width and 170 mm in length. The length of the aluminium film forming a starter crack was about 25 mm. Metallic hinged end tabs, 20 mm long by 20 mm wide, were glued to the ends of the specimens with crack starters as a means of applying the load perpendicular to the interlaminar layer. One edge of each specimen was coated with white correction fluid and marked at about 2 mm intervals to aid visually locating the crack tip.

An Instron 1121 test machine was used to load the fracture specimens in mode I. No effort was made to produce a "natural precrack", and the specimens were loaded in continuous monotonic fashion at a crosshead speed of 2 mm min^{-1}. The load and displacement were recorded continuously in an x–y plotter. The crack growth was observed in the specimen edge using a travelling microscope. When the tests were finished, the DCB fracture surfaces were examined directly, after gold coating, in a Jeol JXA-840 scanning electron microscope (SEM).

The fracture toughness determination for the DCB specimens was performed by using the experimental compliance calibration method proposed by Berry [8]:

$$C = Ka^n \quad (1)$$

where C is the compliance, a the measured crack length, and K and n are empirical parameters. The mode I fracture toughness G_{IC} is then given by

$$G_{IC} = nP\delta/2ba \quad (2)$$

where P and δ are the critical load and displacement, respectively, at crack length a, and b is the width of the DCB specimen.

2.3. Interlaminar shear strength

In order to assess the fibre wetting and fibre–matrix adhesion, interlaminar shear strength tests were conducted at room temperature in accordance with ASTM D-2344 by using a three-point loading fixture with a constant span-to-depth ratio of 4. The rate of loading was 2 mm min^{-1}. From ASTM D-2344, the interlaminar shear strength (ILSS) is given by

$$\text{ILSS} = 3P/4bh \quad (3)$$

where h is the sample thickness. The test is valid only if the sample fails in shear.

2.4. Dynamic mechanical analysis

A Du Pont 9900 instrument was used at a heating rate of 5 °C min^{-1} to measure the glass transition temperatures (the flexural loss modulus peaks) of the three composites.

3. Results

From load–displacement curves for DCB specimens of the three materials linear elastic responses were observed. At the point of deviation from linearity, subcritical crack growth occurred from the aluminium foil. When the load reached a maximum the interlaminar crack grew in a continuous, stable manner through the specimen until the crack length was about 80 mm. During the crack propagation, no obvious fibre bridging behind the crack tip was observed from side views of the three composites.

Based on the load–displacement traces and corresponding crack lengths, the relationship between compliance and crack length can be obtained. By the use of the linear regression analysis, the exponent n in Equation 1 is determined. The results for three composites are listed in Table I (the correlation coefficients are also given, which indicates an excellent fit). The interlaminar fracture toughness G_{IC} is then calculated from Equation 2 for each composite.

Variations of the interlaminar fracture toughness with crack growth (R curves) for the three composites are shown in Fig. 1. Values of G_{IC} (init) were evaluated corresponding to the crack initiation point determined by the deviation from the linear slope of the load–displacement curve. From Fig. 1, it is interesting to find that the R curves of these three composites were different from each other not only in the initial toughness but also on the steady-state or plateau toughness at long crack lengths. For CTU4/PTI (A), G_{IC} increased from the starter crack length and then levelled off at a value nearly twice as high as the initiation value. This is a commonly observed feature in these tests [9, 10]. For CTU4/PTI (B), after a rapid small rise from the crack starter film, the G_{IC} reached a peak at low crack length and then descended and

TABLE I Values of the Berry exponent

Material	Berry exponent	Correlation coefficient
CTU4/PTI (A)	2.75	0.9986
CTU4/PTI (B)	2.59	0.9990
CTU4/PTI (C)	2.78	0.9992

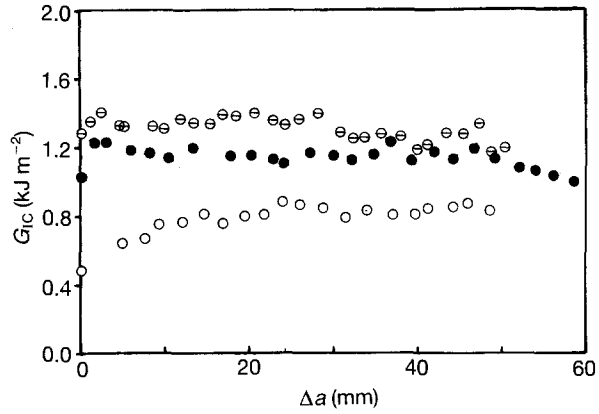

Figure 1 Mode I R curves: (○) CTU4/PTI (A), a_o = 25.26 mm; (●) CTU4/PTI (B), a_o = 26.94 mm; (⊖) CTU4/PTI (C), a_o = 24.86 mm.

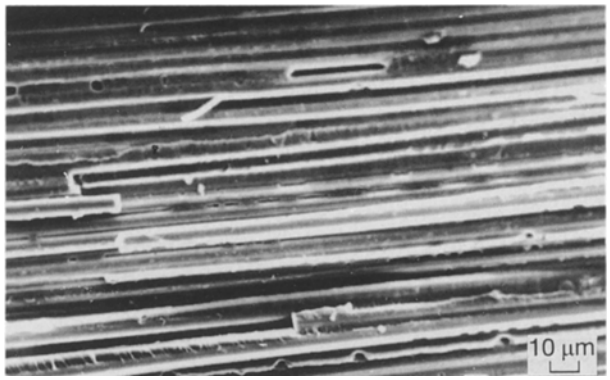

Figure 2 Scanning electron micrograph of CTU4/PTI (A) fracture surface.

Figure 3 Scanning electron micrograph of CTU4/PTI (B) fracture surface.

levelled off at long crack lengths. However, for CTU4/PTI (C) no obvious R curve is revealed.

Typical micrographs of fracture surfaces for these materials are shown in Figs 2 to 4. It can be seen that for all three composites there were no disturbed fibres on the fracture surface and fibres were almost coated with the matrix resin, indicating that the fibres were wetted sufficiently by the matrix and fibre–matrix adhesion was good. It was observed that there were differences in both the amount of surface roughness and the number of broken fibres per unit

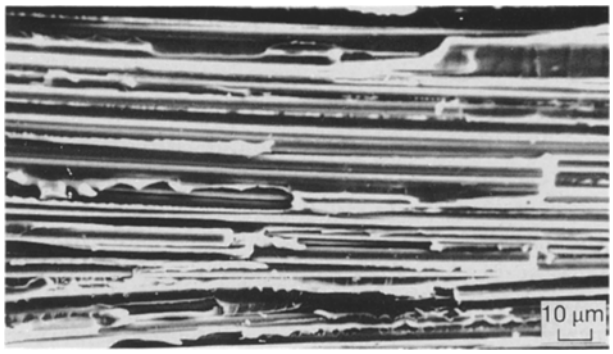

Figure 4 Scanning electron micrograph of CTU4/PTI (C) fracture surface.

TABLE II Summary of ILSS and T_g data for the composites

Material	ILSS (MPa)	T_g (°C)
CTU4/PTI (A)	99	262
CTU4/PTI (B)	97	266
CTU4/PTI (C)	97	258

area among these three composites. For CTU4/PTI (A), the fracture surface was relatively smooth with the matrix showing fewer signs of ductility. The fracture surface of CTU4/PTI (B) was somewhat similar to that of CTU4/PTI (C), this similarity being reflected in the approximate agreement of the toughness values for crack propagation.

The results of short beam tests for measuring the ILSS and dynamic mechanical analysis for measuring the glass transition temperature T_g of these three materials are summarized in Table II.

4. Discussion

4.1. Analysis of fracture toughness

Interlaminar fracture in a unidirectional composite is a complicated process which involves the fracture of matrix resin, peeling of fibres, debonding of the matrix–fibre interface, breakage of bridging fibres and extension of a damage zone. The steady-state propagation toughness value includes contributions from all these sources and the total toughness is therefore given by

$$G_{IC}^{c} = G^{m} + G^{p} + G^{d} + G^{b} + G^{o} \quad (4)$$

where G_{IC}^{c} is the composite fracture toughness; G^{m} is the contribution from deformation and fracture of the matrix; G^{p}, G^{d} and G^{b} are the contributions from fibre peeling, fibre–matrix debonding and fibre breakage, respectively; G^{o} is other energy dissipations per unit area. In the present study it will be assumed that G^{o} is negligible. The interlaminar toughness is expected to increase with an increase in any of the above quantities.

The contribution from peeling fibres, G^{p}, can be derived from a model present by Crick *et al.* [11] based on the assumption that the energy dissipation

for matrix resin fracture and deformation in peeling fibres is the same as that in crack propagation:

$$G^{p} = G^{m}\pi r n_{p} l_{p} \quad (5)$$

where r is the mean radius of the fibres, n_p the number of peeling fibres per unit area and l_p the average peeling length of the fibres.

By analogy,

$$G^{d} = W_{a} 2\pi r n_{a} l_{a} \quad (6)$$

where W_a is the interfacial work of fracture, n_a the number of debonded fibres per unit area at fracture surface and l_a the average debonding length.

It can be imagined that fibre peeling and fibre–matrix debonding are two failure mechanisms which compete in the interlaminar fracture process. The increase in absorbed energy due to debonding is at the expense of the contribution from matrix deformation and fracture due to peeling. Their contributions to the total toughness will depend on the balance between these two mechanisms.

The energy dissipation due to fibre breakage can be estimated from the maximum amount of stored elastic energy per unit volume in a fibre and the exposed length of broken fibre, l_b, and the number of broken fibres per unit area at fracture surface, n_b:

$$G^{b} = \frac{1}{2}\sigma\varepsilon\pi r^{2} n_{b} l_{b} \quad (7)$$

where σ is the fibre fracture stress and ε the fibre fracture strain.

From the above analysis it can be seen that the interlaminar fracture toughness of a composite is not controlled by a single material parameter, but is dependent on its constituents and their complex interaction.

In the present study, the very similar values of interlaminar shear strength for the three composites suggest that fibre wetting and fibre–matrix adhesion in these materials are roughly identical. Observations of fracture surfaces reveal that few debonded fibres are found in the three composites. These results show that good fibre wetting and fibre–matrix adhesion are attained in CTU4/PTI. Thus, it can be thought that there is no contribution from the fibre–matrix debonding in the composite fracture toughness ($n_a = 0$, $l_b = 0$). However, there is evidence of peeled and broken single fibres on the fracture surface. Examinations show that the bridging fibres in these composites peel over short distances and break, so it is reasonable to assume that the number of peeling fibres is the same as that of broken fibres; the average peeling length of the fibres is then equal to the average length of the fibres at breakage, i.e. $n_p = n_b = n$, $l_p = l_b = l$. The quantity n for the three composites can be estimated from visual analysis of fracture surfaces, but the uncertainty in the mean values is considerable. For CTU4/PTI (A), CTU4/PTI (B), CTU4/PTI (C), the numbers of broken fibres per square metre of fracture surface are $5.7 \pm 2.3 \times 10^{7}$, $5.7 \pm 3.2 \times 10^{7}$ and $8.2 \pm 4.6 \times 10^{7}$, respectively. Because it is very difficult to obtain the mean value of peeling length from fracture surfaces, in order to evaluate the contributions of G^p and G^b it is assumed that $l = 0.5$ mm. Investigations of fracture surfaces indicate that this value may be the upper limit of peeling lengths.

Based on values adopted from the data sheet of the supplier of CTU4 carbon fibre ($\sigma = 3.6$ GPa, $\varepsilon = 0.013$, $r = 3.5$ μm), G^b in the three composites was calculated from Equation 7. The values obtained are about 0.01 kJ m^{-2}, which is very small compared to the total toughness and so can be ignored. By analogy, G^p is estimated by using Equations 5. It is found that the contribution of fibre peeling to the total toughness for interlaminar fracture is approximately $0.31G^m$ to $0.45G^m$ in the three composites. During crack initiation from the crack starter foil there is no fibre peeling ($n_p = 0$); the fracture toughness, G^c_{IC} (init), results mainly from deformation and fracture of the matrix, G^m, i.e. G^c_{IC} (init) = G^m.

From the discussion so far different failure mechanisms have been separated and a quantitative approach has been used to evaluate the various contributions. For the CTU4/PTI materials studied here, it is apparent that deformation and fracture of the matrix make a significant contribution to the interlaminar fracture toughness, and the contributions from fibre–matrix debonding and fibre breakage can be neglected.

According to the results of the above analysis, G^c_{IC} (prop) of CTU4/PTI can be written as

$$G^{c}_{IC}(\text{prop}) = G^{c}_{IC}(\text{init})(1 + \pi r n_{p} l_{p}) \quad (8)$$

For CTU4/PTI (A), G^c_{IC} (init) = 0.48 kJ m^{-2} and $\pi r n_p l_p = 0.31$, which yields G^c_{IC} (prop) = 0.63 kJ m^{-2}. However, the measured value of G^c_{IC} (prop) in CTU4/PTI (A) is 0.82 kJ m^{-2}. Though the peeling length, $l = 0.5$ mm, is an assumption, our observations show that this length may be the largest one. There must therefore be some other energy dissipations during interlaminar fracture. Possible processes may be the formation of microcracks in the interfacial region, and side cracks and crack branches around the main crack tip. Fig. 5 shows an observed crack branch from the fracture surface of CTU4/PTI (A). On the other hand for CTU4/PTI (C) G^c_{IC} (init) is almost the same as the measured G^c_{IC} (prop) (see Fig. 1), so Equation 8 obviously gives an overestimated value of G^c_{IC} (prop). A likely reason may be the larger assumed l_p value.

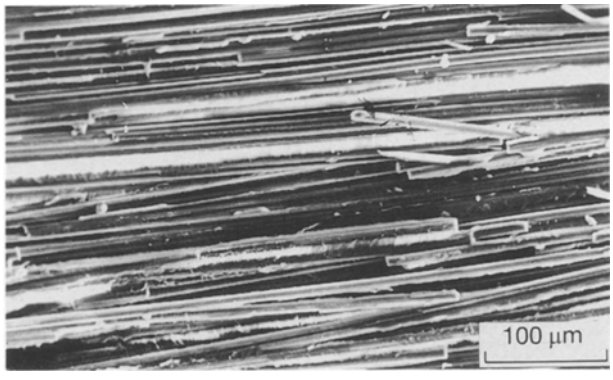

Figure 5 Crack branch from fracture surface CTU4/PTI (A).

Thus, in order to make an accurate quantitative comparison between the contributory failure mechanisms, the parameters in the models must be known with some confidence.

4.2. Matrix ductility

There is an interesting problem emerging from this investigation, i.e. that the values of measured G_{IC}^{c} (init) and G_{IC}^{c} (prop) of the three composites are different from each other. From the above discussion, it can be seen that G_{IC}^{c} (init) is dominated by G^{m}. In general G^{m} is not coincident with the fracture toughness of the bulk matrix resin G^{r}, but is significantly related to it. Another factor, which will influence G^{m}, is the fibres constraints to the size of the plastic zone of the matrix. Variations of values of G_{IC}^{c} (init) may therefore arise from two causes. The first is the differences in the resin–rich region at the crack starter which have been observed at fracture surfaces; this results in differences in development of the plastic deformation zone. The second is that the fracture toughness of the matrix resin, G^{r}, may be not alike in the three composites. SEM examinations, which show that the matrix resins in CTU4/PTI (B) and CTU4/PTI (C) are apparently more ductile than the matrix in CTU4/PTI (A) (see Figs 2 to 4), provide support for this view.

It should be pointed out that the monomers in the three composites are exactly the same, and the processing conditions of condensation and consolidation are identical during manufacture of these materials. The only difference is in the reactant solutions, which were prepared by using three different alkyl alcohols. It can be imagined that esterification in the three reactant solutions may be different because of variations between the alcohol solvents. However, this should not influence the polymerization of PTI, which has been identified by infrared spectra following the condensation reaction [12]. Th approximate values of T_g for three composites (see Table II) suggest that the extent of polymerization of monomeric reactants are nearly equal in these materials. Thus, there is no reason to believe that the fracture toughnesses of the matrix in the three composites are not alike. However, the actual results of the present study of composites seemingly do not conform to this. Since it is not possible to measure the fracture toughness of the matrix resin at this moment, this problem is left for further investigation.

5. Conclusions

Based on the results in this study the following conclusions can be drawn.

1. Monomeric reactant solutions prepared from different alkyl alcohol solvents have no influence on the fibre wetting and fibre–matrix adhesion in CTU4/PTI composites.
2. The interlaminar fracture toughnesses of each of the materials, namely CTU4/PTI (A), CTU4/PTI (B), CTU4/PTI (C), are not alike, not only in propagation value but also in initial value.
3. SEM examinations provide experimental evidence of variations in matrix ductility of the three composites, but these should be further identified by other studies.
4. Several processes are seen to occur in the interlaminar fracture of the investigated materials. These include matrix fracture and deformation, fibre peeling and fibre breakage. The quantitative approach to microscopy has enabled a calculation of the contributions from the different processes, but there are a number of simplifying assumptions. It is believed that interlaminar fracture in CTU4/PTI is primarily controlled by fracture and deformation in the matrix. However, in order to understand the interlaminar fracture further and calculate the contributions from the other processes accurately, it is necessary to develop and perfect the quantitative approach for assessing various failure mechanisms.

References

1. J. M. WHITNEY, C. E. BROWNING and W. HOOGSTEDEN, *J. Reinf. Plast. Compos.* **1** (1982) 297.
2. P.E. KEARY and L. B. ILCEWICZ, *J. Compos. Mater.* **19** (1985) 154.
3. P. J. HINE, B. BREW, R. A. DUCKETT and I. M. WARD, *Compos. Sci. Technol.* **33** (1988) 35.
4. P. DAVIES, W. CANTWELL, C. MOULIN and H. H. KAUSCH, *ibid.* **36** (1989) 153.
5. S. HASHEMI, A. J. KINLOCH and J. G. WILLIAMS, *J. Mater. Sci. Lett.* **8** (1989) 125.
6. J. ZHOU, T. HE, B. LI, W. LIU and T. CHEN., *Compos. Sci. Technol.* **45** (1992) 173.
7. J. KIM, C. BAILLIE, J. POH and Y. W. MAI, *ibid.* **43** (1992) 283.
8. J. P. BERRY, *J. Appl. Phys.* **34** (1963) 62.
9. S. HASHEMI, A. J. KINLOCH and J. G. WILLIAMS, *J. Compos. Mater.* **24** (1990) 918.
10. L. YE and K. FRIEDRICH, *J. Mater. Sci. Lett.* **11** (1992) 1537.
11. R. A. CRICK, D. C. LEACH, P. J. MEAKIN and D. R. MOORE, *J. Mater. Sci.* **22** (1987) 2094.
12. J. ZHOU, T. HE. J. ZHANG and M. DING, unpublished data (1993).

Received 25 May
and accepted 8 October 1993